

---

Original Paper

---

# Improving Flow Distribution in a Suction Channel for a Highly Efficient Centrifugal Compressor

Manabu Yagi<sup>1</sup>, Takanori Shibata<sup>1</sup>, Hiromi Kobayashi<sup>2</sup>, Masanori Tanaka<sup>2</sup> and Hideo Nishida<sup>2</sup>

<sup>1</sup>Hitachi Research Laboratory, Hitachi, Ltd.

832-2 Horiguchi, Hitachinaka-shi, Ibaraki, 312-0034, Japan  
manabu.yagi.cb@hitachi.com, takanori.shibata.@hitachi.com

<sup>2</sup>Tsuchiura Research Laboratory, Hitachi Plant Technologies, Ltd.

603 Kandatsumachi, Tsuchiura-shi, Ibaraki, 300-0013, Japan

hiromi.kobayashi.zm@hitachi-pt.com, masanori.tanaka.ph@hitachi-pt.com, hideo.nishida.cr@hitachi-pt.com

## Abstract

Design parameters for suction channels of process centrifugal compressors were investigated, and an optimization method to enhance stage efficiency by using the new design parameters was proposed. From results of computational fluid dynamics, the passage sectional area ratios  $A_c/A_e$ ,  $A_e/A_s$  and  $A_c/A_s$  were found to be the dominant parameters for the pressure loss and circumferential flow distortion, where  $A_c$ ,  $A_e$  and  $A_s$  are passage sectional areas for the casing upstream side, casing entrance and impeller eye, respectively. The Base suction channel was optimized using the new design parameters, and the Base and Optimized types were tested. Test results showed that the Optimized suction channel achieved 3.8% higher stage efficiency than the Base suction channel while maintaining the same operating range.

**Keywords:** Design parameter, Suction channel, Compressor, Stage efficiency, Circumferential flow distortion

## 1. Introduction

Process centrifugal compressors are widely used in gas processing plants and gas pipelines in the oil and gas industry. These compressors must have a high efficiency and a sufficient operating range because reduction of life cycle costs is a key issue in their application. The installation of compressors having a high efficiency and a wide operating range, can not only reduce power consumption, but also save energy by avoiding bypass operations under a low flow operation.

Many centrifugal compressors in the oil and gas industry are single-shaft multistage types and composed of suction channels, impellers, diffusers, return channels, and discharge scrolls. The suction channel, as shown in Fig. 1, is the subject of the present research. Complex three-dimensional flow fields are formed in the suction channel because intake flow in a radial direction from a suction nozzle is diffused toward the circumferential direction through an annulus flow passage within a casing [1]. Therefore, the circumferential flow distortion, which has an unfavorable influence on internal flow of the downstream side impeller, is generated in the flow fields of the casing. This indicates that, not only decreasing the pressure loss in the suction channel but reducing the circumferential flow distortion at the impeller inlet also have possibilities to improve the impeller efficiency.

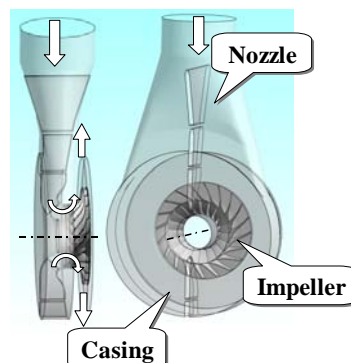


**Fig. 1** Geometry and main dimensions of the suction channel

The design parameters of the suction channels in centrifugal pumps which reduce the flow distortion have already been presented [2]. However, in centrifugal compressors, a design method using the dominant parameters of the suction channels to improve the compressor performance has not yet been presented, although studies have been done about decreasing the pressure loss [3,4] and evaluating the inlet flow distortion [1,3-7].

Moreover, in the present research, a method for optimizing the suction channel design to enhance compressor efficiency was investigated by focusing on reducing the circumferential flow distortion at the impeller inlet. This paper discusses the optimization method using design parameters, and also discusses the reasons for increased stage efficiency seen in performance tests.

## 2. Improving Flow Distribution in the Suction Channel

### 2.1 Sensitivity Analysis for Main Dimensions

In order to design highly efficient centrifugal compressors, the main dimensions which determine the configuration of the suction channel for the compressor should be selected suitably. The suction channel for such compressors must have a low pressure loss and circumferential flow distribution which has favorable effects on impeller performance. In order to identify the main dimensions, which have a dominant influence on the pressure loss and circumferential flow distortion, sensitivities of the main dimensions were compared. This sensitivity analysis was carried out for a suction channel with the suction flow coefficient  $\phi_{s,des}=0.125$ . The L18 matrix for the Taguchi method was applied to the eight main dimensions shown in Fig. 2. The control range of the value for the eight main dimensions was determined so as not to create unreal configurations when 18 combinations of dimensions were made. Computational fluid dynamics (CFD) analysis was applied to those 18 cases on only the suction channel without the impeller to evaluate the pressure loss and circumferential flow distortion. In the present study, ANSYS CFX-11™ was used to solve the Reynolds-averaged Navier-Stokes equations (RANS) numerically with the shear stress transport (SST) turbulence model at the steady state for the CFD analysis. All cases of the CFD calculating regions were circumferential half sectors of the suction channel, which was divided by the flow dividing plate along the vertical centerline as shown in Fig. 3. The CFD grid was generated by about 600,000 nodes. Total pressure, total temperature and normal flow direction at the nozzle inlet were specified as the inlet boundary conditions. Mass flow rate at the outlet CFD region was specified as the outlet boundary condition.

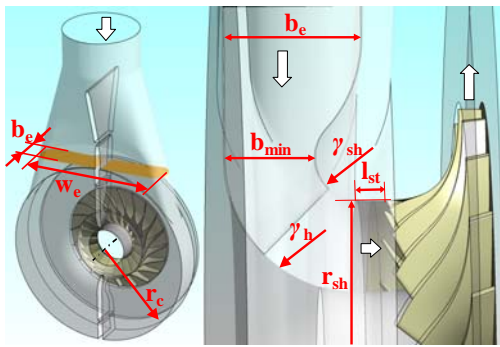


Fig. 2 Main dimensions of the suction channel

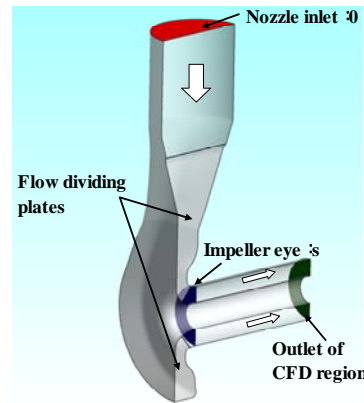


Fig. 3 CFD calculating region of the half sector model

In the present study, the total pressure loss coefficient  $\zeta_{sc}$  and the maximum swirl angle  $\alpha_{s,max}$  were used as the indicators which evaluated the interior flow field of the suction channel.  $\zeta_{sc}$  was calculated by eq.(1).

$$\zeta_{sc} = \frac{P_{t0} - P_{ts}}{P_{ts} - P_s} \quad (1)$$

$\alpha_{s,max}$  was defined as the maximum value from the mass-averaged swirl angles for six sectors of  $60^\circ$  each at the impeller eye, as shown in Fig. 4.  $\alpha_{s,max}$  had a plus value when the swirl angle was along the rotating direction of the impeller (co-swirl). In the circumferential half sectors of the suction channel as shown in Fig. 3,  $\alpha_{s,max}$  was calculated by using three sectors of  $60^\circ$  each from the vertical centerline.

The signal-to-noise ratios (SN ratios) of each main dimension for  $\zeta_{sc}$  and  $\alpha_{s,max}$  are shown in Fig. 5. The larger the differences of the SN ratio became, the larger the influence of the control factor on the objective function was. Therefore,  $w_e$  and  $r_c$  had larger influence on  $\zeta_{sc}$ , and  $r_{sh}$  and  $w_e$  had larger influence on  $\alpha_{s,max}$ . The right plotted points of each dimension were larger than the left ones, and the larger points of the SN ratio could reduce the objective functions  $\zeta_{sc}$  and  $\alpha_{s,max}$ . This indicated that larger  $w_e$  and smaller  $r_c$  were effective for decreasing  $\zeta_{sc}$ , and that larger  $w_e$  and smaller  $r_{sh}$  were necessary for decreasing  $\alpha_{s,max}$ . From these results, increasing the decelerated ratio of flow velocity from the casing entrance section  $e$  to the upstream side  $c$  was considered to reduce  $\zeta_{sc}$ . Increasing the accelerated velocity ratio from the section  $e$  to the impeller eye section  $s$  was also considered to reduce  $\alpha_{s,max}$ .

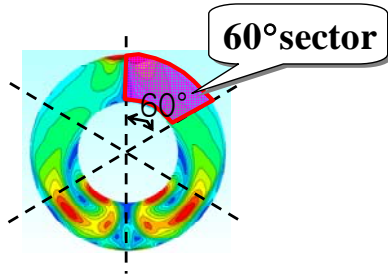


Fig. 4 60°sectors at impeller eye

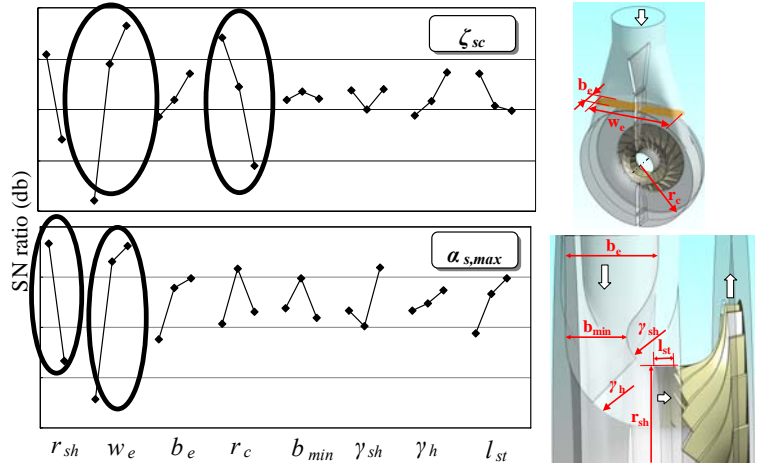


Fig. 5 Sensitivities of main dimensions to pressure loss  $\zeta_{sc}$  and maximum swirl angle  $\alpha_{s,max}$  with  $\phi_{s,des}=0.125$

## 2.2 Identified Non-dimensional Design Parameters

It was determined that the main dimensions  $w_e$ ,  $r_c$  and  $r_{sh}$  had high sensitivity against  $\zeta_{sc}$  and  $\alpha_{s,max}$  at  $\phi_{s,des}=0.125$ . However, finding the non-dimensional design parameters, which can be used consistently for various sizes and shapes of the suction channel, is required because process centrifugal compressors are designed with a wide range of  $\phi_{s,des}$ . In order to satisfy this requirement, the correlations of the normalized design parameters, such as the main dimension ratios and sectional area ratios, with  $\zeta_{sc}$  and  $\alpha_{s,max}$  were investigated. Eighteen cases of CFD results at  $\phi_{s,des}=0.125$  (Fig. 5) were utilized to find the normalized parameters. The normalized design parameters including  $w_e$ ,  $r_c$  and  $r_{sh}$ , which had large influence on  $\zeta_{sc}$  and  $\alpha_{s,max}$ , were surveyed.

It was clear from Fig. 6 that the passage sectional area ratio  $A_c/A_e$  correlated with  $\zeta_{sc}$ , and that  $A_e/A_s$  and  $A_c/A_s$  correlated with  $\alpha_{s,max}$ .  $A_c$ ,  $A_e$  and  $A_s$  are passage sectional areas for the casing upstream side  $c$ , casing entrance  $e$  and impeller eye  $s$ , respectively, as also shown in Fig. 6. Each horizontal axis in Fig. 6 was normalized by the values of the Base suction channel with  $\phi_{s,des}=0.1$  (Base). The correlation between  $A_c/A_e$  and  $\zeta_{sc}$  revealed that a smaller  $A_c/A_e$  decreased  $\zeta_{sc}$ . This indicated that reducing the expansion ratio of the passage sectional area from  $A_e$  to  $A_c$  by enlarging  $A_e$  to bring it close to  $A_c$  could decrease  $\zeta_{sc}$ .

The correlation of  $A_e/A_s$  and  $A_c/A_s$  with  $\alpha_{s,max}$  revealed that larger  $A_e/A_s$  and  $A_c/A_s$  decreased  $\alpha_{s,max}$ . From these correlations, two procedures were considered possible for decreasing  $\alpha_{s,max}$ . One enlarged  $A_e$  in order to obtain sufficient deceleration from the nozzle inlet  $\theta$  to the entrance of the casing passage  $e$  and to spread the flow in the circumferential direction through the annulus casing passage. The other enlarged  $A_c$  in order to obtain proper acceleration from the casing upstream side passage  $c$  to the impeller eye  $s$ . This acceleration was considered to be effective for concentrating the flow with radial inflow direction from the annulus casing passage and decreasing the velocity ratio of the tangential to axial directions at the impeller eye  $s$ .

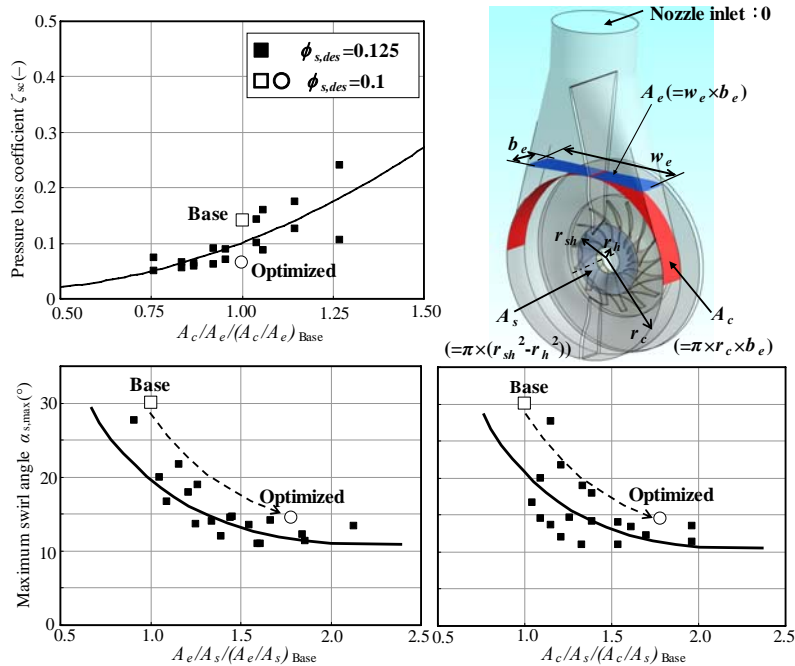


Fig. 6 Correlations between design parameters and pressure loss  $\zeta_{sc}$  and maximum swirl angle  $\alpha_{s,max}$  in Base and Optimized suction channels

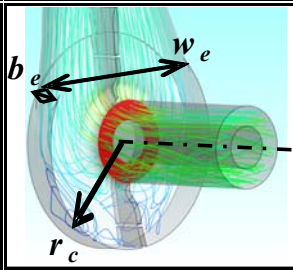
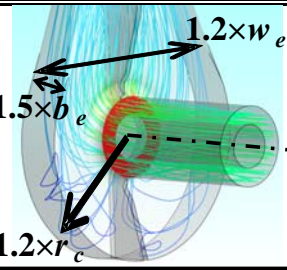
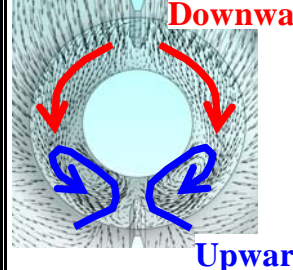
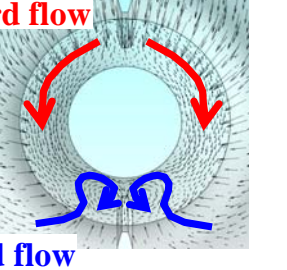
### 2.3 Improvements Resulting from Optimization

Confirming the effectiveness of these three design parameters  $A_c/A_e$ ,  $A_e/A_s$  and  $A_c/A_s$  with  $\phi_{s,des} \neq 0.125$  is also necessary since process centrifugal compressors are designed at various  $\phi_{s,des}$ . Therefore, the following three steps were carried out. First, the shape of the Base suction channel with  $\phi_{s,des}=0.1$  ( $\square$  in Fig. 6) was optimized to reduce  $\zeta_{sc}$  and  $\alpha_{s,max}$  by using the correlation maps with  $\phi_{s,des}=0.125$ . Second, the reduction of  $\zeta_{sc}$  and  $\alpha_{s,max}$  by optimizing the Base suction channel were confirmed in the CFD results. Third, increase of the compressor stage efficiency for the Optimized suction channel was evaluated by testing both types.

In the first step, both  $A_e/A_s$  and  $A_c/A_s$  of the Base suction channel were increased to 1.8 ( $\circ$ , Optimized in Fig. 6) with expected reduction of  $\alpha_{s,max}$ . In this case,  $A_c/A_e$  was retained because increasing ratios of  $A_e$  and  $A_c$  were almost the same. The Optimized suction channel had dimensions of  $1.5 \times b_e$ ,  $1.2 \times w_e$  and  $1.2 \times r_c$  in comparison with the Base suction channel as shown in Table 1. Enlarging  $A_e$  and  $A_c$  was expended to reduce  $\alpha_{s,max}$ , from the correlation curves in Fig. 6, but enlarging  $A_e$  and  $A_c$  should be restricted in order to avoid manufacturing extra-large inlet casing.

In the second step, CFD calculations for the full model of the suction channel only were made to compare the flow fields between the Optimized and the Base suction channels. The computational grid for these CFD calculating regions had about 1.2 million nodes because full model was two times the circumferential half sector model in Fig. 3. Other CFD conditions were already described in Section 2.1. As shown in Table 1, the values of  $\zeta_{sc}$  and  $\alpha_{s,max}$  for the Optimized suction channel were reduced from 0.141 and  $30.1^\circ$  to 0.065 and  $14.5^\circ$ . The reasons for these improvements were considered as follows. The averaged velocity in the casing was decreased due to the increase of both  $A_e/A_s$  and  $A_c/A_s$  for the Optimized suction channel. At the impeller eye in the Optimized suction channel, the tangential velocities of the interaction vortex between the downward flow from the nozzle and upward flow from the bottom side of the casing were also decreased. This effect was considered to result from the decelerated upward flow due to the increase of  $A_c/A_s$  for the Optimized suction channel.

**Table 1** Main dimensions and CFD results for Base and Optimized suction channels

Items	Base	Optimized
<b>Geometry and stream lines</b>		
<b>Tangential velocity vectors around impeller eye</b>		
$\alpha_{s,max}$	<b><math>30.1^\circ</math></b>	<b><math>14.5^\circ</math></b>
$\zeta_{sc}$	<b>0.141</b>	<b>0.065</b>

## 3. Performance Tests

### 3.1 Test Apparatus

In the third step, scaled models of the Base and Optimized suction channels with  $\phi_{s,des}=0.1$  were manufactured and tested, to confirm the increase of compressor stage efficiency resulting from the Optimized suction channel. The test apparatus was composed of a closed loop, and the working gas was circulated [8]. The total pressure and total temperature at the nozzle inlet were maintained at about 101.3 kPa and 293 K, respectively.

A cross section of the model compressor in the test apparatus is shown in Fig. 7. This model compressor mimicked the first stage of a multistage compressor and consisted of a suction channel, impeller, diffuser, and return channel. As the flow distortion at the nozzle inlet  $\theta$  has large influence on the flow uniformity at the impeller eye  $s$  [9], sufficient straight length of a pipe was assembled to maintain uniform flow at the nozzle inlet  $\theta$  in the tests. Only the suction channel was exchanged in the Base and Optimized suction channels while the other components remained the same. A symmetric radial flow passage was also tested as the Uniform case as shown in Fig. 8. The main dimensions of the tested impeller are presented in Table 2.

### 3.2 Measurements and Test Methods

The performance characteristics of the model compressor were obtained by evaluating suction flow coefficients  $\phi_s$ , the efficiencies and head coefficients. The test values of  $\phi_s$  were determined from the volume flow rate of the circulating air, which was measured by an orifice type flow meter based on the Japanese Industrial Standard (JIS). The efficiencies and head coefficients were determined by the total pressures  $P_t$  and total temperatures  $T_t$ , which were measured by Kiel probes and total temperature probes, respectively. Each measurement position is shown in Figs. 7 and 8.

The overall efficiencies and head coefficients were evaluated between the nozzle inlet  $o$  and the stage discharge  $d$ . In addition, the stage efficiencies and head coefficients were also evaluated between the impeller eye  $s$  and the stage discharge  $d$ . In order to break down the loss coefficient of the suction channel only, the difference between overall performance and stage performance was evaluated.

In the tests, air was used as the working gas, and the rotational speed of the impeller was maintained at 17,200 rpm ( $Mu=0.78$ ). The performance characteristics of the model compressors from the maximum flow point to the surge point with the peak of the head coefficient were obtained by changing the opening of a flow control valve.

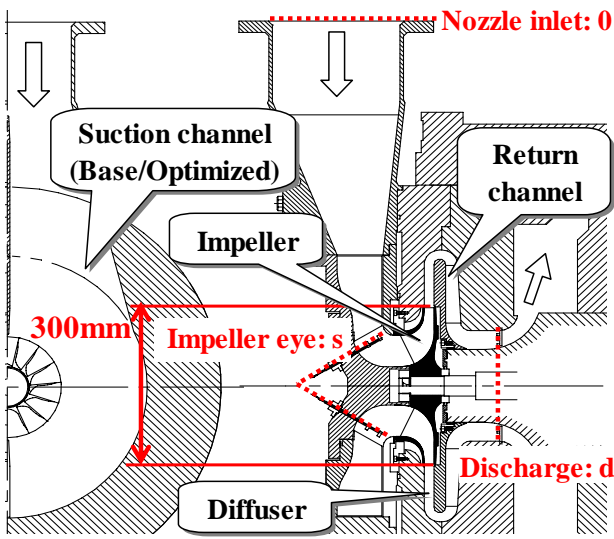


Fig. 7 Cross-sectional view of model compressor with Base or Optimized suction channel

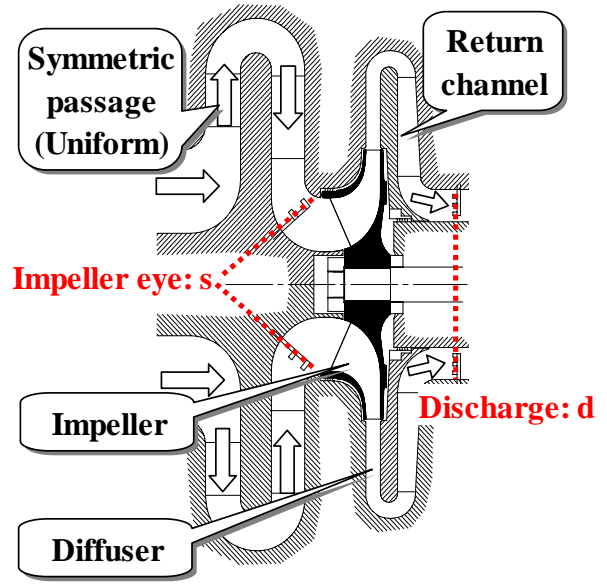


Fig. 8 Cross-sectional view of Uniform case

Table 2 Main dimensions of tested impeller for model compressor

Items		Units	Values
Designed suction flow coefficient	$\phi_{s,des}$	-	0.1
Impeller inlet radius	$r_{sh}$	mm	97
Inlet blade angle at shroud side	$\beta_{1sh}$	°	-60
Inlet blade angle at hub side	$\beta_{1h}$	°	-46
Impeller outlet radius	$r_2$	mm	150

## 4. Test Results and Discussions

### 4.1 Influence of Suction Flow on Overall Performance

Figure 9 shows the measured  $\zeta_{sc}$  and overall performance characteristics between the nozzle inlet  $o$  and the stage discharge  $d$  for the Base and Optimized suction channels. The vertical axes were normalized by the values at the design point in the Base suction channel.  $\zeta_{sc}$  values for the Base and Optimized suction channels were similar at smaller  $\phi_s$  than the design point due to maintaining the dominant parameter  $A_c/A_e$  of  $\zeta_{sc}$  in the present cases. However,  $\zeta_{sc}$  of the Optimized suction channel was decreased from the Base suction channel at larger  $\phi_s$  than the design point. This indicated that the pressure loss could be also decreased at larger  $\phi_s$  when  $A_c/A_e$  and  $A_c/A_s$  were enlarged in order to reduce  $\alpha_{s,max}$ . This result could be accepted in the interdependence of the three design parameters  $A_c/A_e$ ,  $A_e/A_s$  and  $A_c/A_s$ , which is shown by eq. (2).

$$A_c/A_e = A_c/A_s / A_e/A_s \quad (2)$$

The overall efficiency at the design point of the Optimized suction channel was 3.8% higher than that of the Base suction channel while the same operating range from surge to choke was retained. This indicated that the present method of optimization for the suction channel, in which  $A_c/A_e$ ,  $A_e/A_s$ , and  $A_c/A_s$  were determined by using the correlation curves in Fig. 6, was very effective for improving the overall efficiency without reduction of operating range.

#### 4.2 Effect of Improving Flow Distortion on Stage Performance

Figure 10 shows the measured stage performance characteristics between the impeller eye  $s$  and stage discharge  $d$  for the Base, Optimized and Uniform cases. The vertical axes were normalized by the values at the design point in the Base suction channel. The increase in stage efficiency of the Optimized suction channel over that of the Base suction channel was 3.8%, which was the same percentage as the increased overall efficiency. In addition, the performance characteristics of the Optimized suction channel showed good agreement with that of the Uniform case. These results indicated that the main factor increasing the efficiency in the Optimized suction channel was the reduction of  $\alpha_{s,max}$ .

The efficiency drop caused by the pressure loss of the suction channel, that is the difference of efficiency between having and not having a suction channel, was 1.3%. Therefore, the efficiency increase of 3.8% in Fig. 10 was about three times as large as the efficiency drop in the suction channel. This meant that the reduction of  $\alpha_{s,max}$  was more effective for increasing the stage efficiency than reduction of the pressure loss in the suction channel.

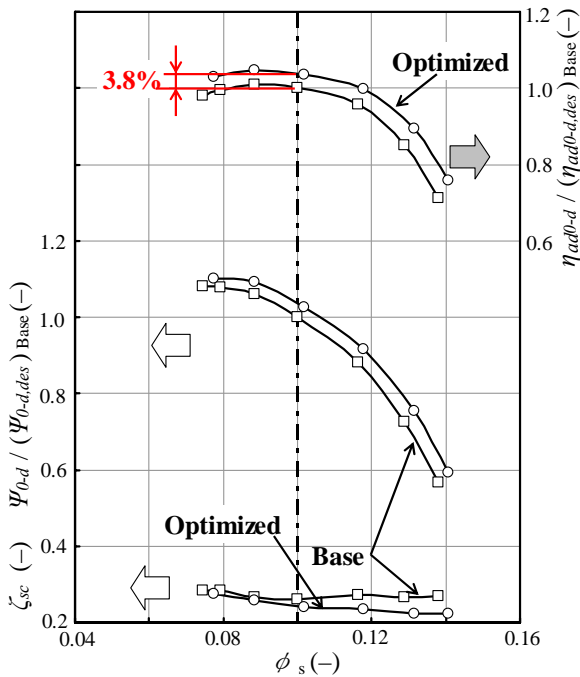


Fig. 9 Measured overall performance characteristics

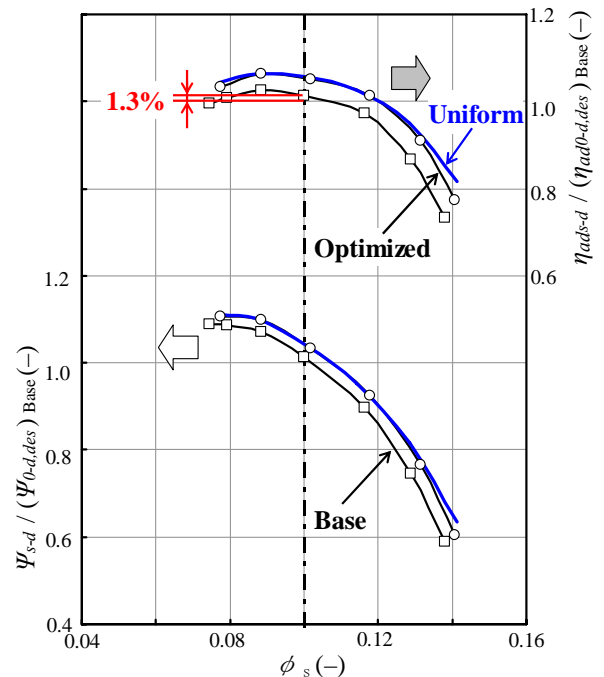


Fig. 10 Measured stage performance characteristics

#### 4.3 Principal Factors for Improving Flow Distortion

The test results revealed that the efficiency of the Optimized suction channel was increased over that of the Base suction channel. In order to clarify the physical mechanisms of this improved performance, CFD numerical analyses for the circumferential flow distribution were conducted.

First, the circumferential distribution of the swirl angle  $\alpha_s$ , total pressure  $P_{ts}$  and mass flow rate  $m$  at the impeller eye were obtained from the CFD results for the full model of the suction channel only in the Base and Optimized suction channels, as shown in Fig. 11. The plotted values were the mass-averaged values for six sectors of  $60^\circ$  each at the impeller eye, and  $P_{ts}$  and  $m$  were normalized by the mass-averaged value of the full model for the Base suction channel. The reductions of both circumferential flow distortion and pressure loss in the Optimized suction channel were observed in Fig. 11 since  $\alpha_s$  and  $P_{ts}$  for the Optimized suction channel were reduced to nearly  $0^\circ$  and increased, respectively, in comparison with the Base suction channel. Anyway, the increases of  $m$  at the  $0-60^\circ$  and  $300-360^\circ$  sectors for the Optimized suction channel were also revealed. These increases of  $m$  were considered to have unfavorable effects because meridional velocities were increased, but their influences were small enough not to decrease the impeller efficiency as told in the following description.

Second, the  $\alpha_s$ ,  $P_{ts}$  and  $m$  at the impeller eye in each  $60^\circ$  sector (Fig. 11) were used as the input boundary conditions of CFD; and the one passage sector model for the combination of the uniform axial inflow passage and tested impeller was used as shown in Fig. 12. The efficiencies and relative velocities  $w_1$  of each  $60^\circ$  sector in Fig. 13 were calculated using the CFD model in Fig. 12. The vertical axes were also normalized by the mass-averaged values of the Base suction channel. Not only increasing efficiencies but also decreasing relative velocities over the Base suction channel could be seen in the  $180-360^\circ$  sector. This  $180-360^\circ$  sector with improved efficiency corresponded to the counter-swirl flow region with  $\alpha_s < 0^\circ$  in Fig. 11.

Third, the differences of the deformed inlet velocity triangles between co-swirl and counter-swirl flow were examined in Table 3, where  $\alpha_s$  was utilized to represent  $\alpha_1$  because  $\alpha_s$  correlated with  $\alpha_1$ . When the counter-swirl flow occurred,  $w_1$  decreased as the absolute value of  $\alpha_1$  became smaller. In addition, the loss caused by increase of incidence angle  $i_1$  was also reduced as  $\alpha_1$

approached  $0^\circ$ . Decreased  $w_l$  and  $\alpha_l$  were considered to be the main factors for improving impeller efficiency. On the other hand, in the co-swirl flow region with  $\alpha_s > 0^\circ$ , while  $w_l$  increased as the absolute value of  $\alpha_l$  became smaller,  $i_l$  decreased at the same time. As a result, efficiency drops could not be observed in the  $0$ - $180^\circ$  sector with the co-swirl flow although  $w_l$  was increased.

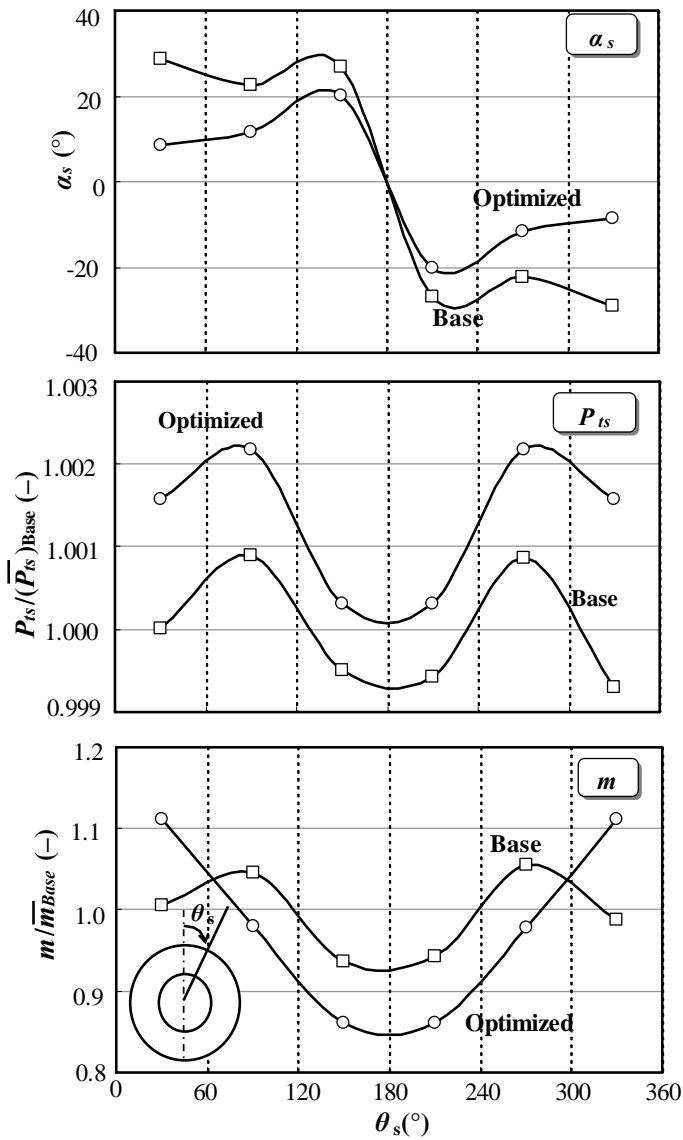


Fig. 11 Circumferential flow distribution obtained by  $60^\circ$  sectors for full model of suction channel only

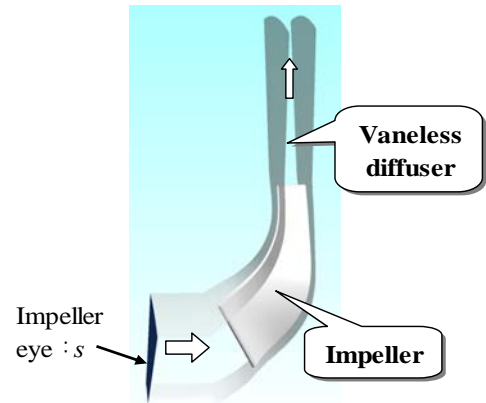


Fig. 12 CFD calculating region of the one passage model

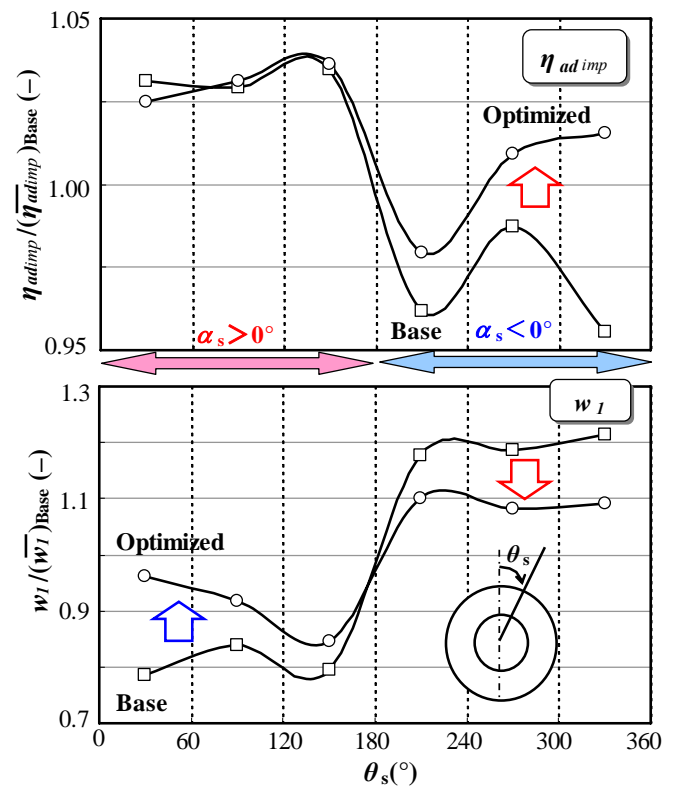


Fig. 13 Circumferential flow distribution obtained by CFD results for one passage models

Table 3 Deviations of inlet velocity triangles caused by inlet swirl

Swirl direction	$\alpha_s > 0^\circ$	$\alpha_s < 0^\circ$
Inlet velocity triangle		
Absolute value of swirl angle $ \alpha_l $	↓	↓
Relative velocity $w_l$	↑	↓
Incidence angle $i_l$	↓	↓
Impeller efficiency $\eta_{imp}$	→	↑

↑ : Increase, ↓ : Decrease, → : Unchanged

## 5. Conclusion

The Base suction channel was optimized by using newly presented design parameters. Both the Optimized and Base suction channels were tested to evaluate the performance enhancement using the optimization method at a suction flow coefficient of 0.1. Specific conclusions can be summarized as follows.

(1) Based on the results of analyzing the sensitivity of main dimensions to the pressure loss and swirl angle, the passage sectional area ratios  $A_c/A_e$ ,  $A_c/A_s$  and  $A_e/A_s$  were identified as the design parameters for the suction channel, where  $A_c$ ,  $A_e$  and  $A_s$  are passage sectional areas for the casing upstream side, casing entrance and impeller eye, respectively.  $A_c/A_e$  had a strong correlation with the pressure loss. Both  $A_c/A_s$  and  $A_e/A_s$  were dominant parameters for the circumferential flow distortion.

(2) By revising the two passage sectional area ratios  $A_c/A_s$  and  $A_e/A_s$ , the compressor stage efficiency was increased by 3.8% in comparison with the Base suction channel and the overall operating range from surge to choke was retained. From this test result, the optimization method using correlation curves of the pressure loss and circumferential flow distortion to the above-mentioned three design parameters was demonstrated as very effective to improve the compressor performance. Therefore, the three design parameters were newly presented as the dominant design parameters for the suction channel.

(3) Test results clearly showed that the 3.8% higher efficiency than that of the Base suction channel was achieved by improving the circumferential flow distortion at the impeller eye. Test results also showed that the efficiency drop due to the circumferential flow distortion at the impeller eye was three times larger than that of the total pressure loss in the suction channel. Hence, reducing the circumferential flow distortion was more effective for improving the stage efficiency than decreasing the pressure drop in the present study.

(4) From numerical analyses, the decreases of both the relative velocity and incidence angle at the impeller inlet in the counter-swirl flow region were considered to be the main factors for improving impeller efficiency.

## Acknowledgments

The authors wish to express their appreciation to Hitachi Laboratory in Hitachi, Ltd., Tsuchiura Laboratory and Tsuchiura Works in Hitachi Plant Technologies, Ltd., and American Society of Mechanical Engineers for permission to publish this paper. They also thank Dr. Y. Fukushima in Hitachi Plant Technologies, Ltd. for his technical assistance during this investigation.

## Nomenclature

$a$	Velocity of sound [m/s]	$\eta$	Total to total efficiency [%]
$A$	Passage sectional area [m <sup>2</sup> ]	$\theta$	Circumferential coordinate [°]
$b$	Axial width of passage [m <sup>2</sup> ]	$\psi$	Head coefficient ( $=H_{ad}/u_2^2$ )
$b_{min}$	Minimum axial width of passage [m <sup>2</sup> ]	$\zeta$	Total pressure loss coefficient
$c$	Absolute velocity [m/s]	<b>Subscripts</b>	
$H_{ad}$	Adiabatic head [m]	$0$	Nozzle inlet
$i$	Incidence angle [°]	$e$	Entrance of casing passage
$l_{st}$	Axial length of straight passage [m]	$c$	Casing upstream side passage
$Mu$	Peripheral Mach number ( $=u_2/a$ )	$s$	Impeller eye
$Q$	Volume flow rate [m <sup>3</sup> /s]	$l$	Leading edge of impeller
$P_t$	Total pressure [Pa]	$2$	Impeller exit
$r$	Radius [m]	$ad$	Adiabatic condition
$r_c$	Inside radius of casing [m]	$des$	Design point
$u$	Peripheral velocity [m/s]	$h$	Hub side
$w_l$	Impeller inlet relative velocity [m/s]	$imp$	Impeller
$w_e$	Horizontal width at entrance of casing [m]	$m$	Meridional direction
$\alpha$	Swirl angle from meridional direction [°]	$max$	Maximum value
$\beta$	Relative flow angle from meridional direction [°]	$sh$	Shroud side
$\beta_b$	Impeller blade angle [°]	<b>Subscripts</b>	
$\phi$	Suction flow coefficient ( $=Q_s/\pi r_2^2 u_2$ )		Absolute value
$\gamma$	Radius of curvature [m]	-	Mass-averaged value

## References

- [1] Flathers, M. B., Bache, G. E. and Rainsberger, R., 1994, "An Experimental and Computational Investigation of Flow in a Radial Inlet of an Industrial Pipeline Centrifugal Compressor," ASME Paper 94-GT-134.
- [2] Gülich, J. F., 2008, Centrifugal Pumps: Section 7.13, Springer, Berlin.
- [3] Pazzi, S. and Michelassi, V., 2000, "Analysis and Design Outlines of Centrifugal Compressor Inlet Volute," ASME Paper 2000-GT-464.
- [4] Kim, Y. and Koch, J., 2004, "Design and Numerical Investigation of Advanced Radial Inlet for a Centrifugal Compressor Stage," IMECE 2004-60538.
- [5] Lüdtke, K. H., 2004, Process Centrifugal Compressors, Springer, Berlin.
- [6] Ariga, I., Kasai, N., Masuda, S., Watanabe, Y. and Watanabe, I., 1983, "The Effect of Inlet Distortion on the Performance Characteristics of a Centrifugal Compressor," Transactions of the ASME: J. of Eng. for Power, Vol. 105, pp. 223-230.
- [7] Kim, Y., Engeda, A., Aungier, R. and Direnzi, G., 2001, "The Influence of Inlet Flow Distortion on the Performance of a

Centrifugal Compressor and the Development of an Improved Inlet using Numerical Simulations,” *Imech E: J. of Power and Energy*, Vol. 215, Part A, pp. 323-338.

[8] Yagi, M., Kishibe, T., Shibata, T., Nishida, H. and Kobayashi, H., 2008, “Performance Improvement of Centrifugal Compressor Impellers by Optimizing Blade-Loading Distribution,” ASME Paper GT2008-51025.

[9] Koch, J., Chow, P., Hutchinson, B. and Elias, S., 1995, “Experimental and Computational Study of a Radial Compressor Inlet,” ASME Paper 95-GT-82.